Amyloid Fibrils

DOI: 10.1002/anie.201100807

Direct Observation of Time-Resolved Polymorphic States in the Self-Assembly of End-Capped Heptapeptides

Jozef Adamcik, Valeria Castelletto, Sreenath Bolisetty, Ian W. Hamley, and Raffaele Mezzenga**

Amyloid fibrils resulting from uncontrolled peptide aggregation are associated with several neurodegenerative diseases.[1–6] Their polymorphism depends on a number of factors including pH, ionic strength, electrostatic interactions, hydrophobic interactions, hydrogen bonding, aromatic stacking interactions, and chirality.[7–17] Understanding the mechanism of amyloid fibril formation can improve strategies towards the prevention of fibrillation processes and enable a wide range of potential applications in nanotemplating and nanotechnology.[18–22]

In β-sheet-driven self-assembly of peptides and proteins, several transient polymorphic states of the fibrillation process have been reported. In heat-denaturated β-lactoglobulin amyloid fibrils, the transition of single protofilaments into multistranded twisted ribbons was reported and rationalized in terms of liquid-crystalline, hydrophobic, and electrostatic interactions.[23] Further evolution of the final multistranded twisted-ribbon structure appeared to be quenched by the strong interactions associated with long peptide sequences specific to this system.[8] However, for shorter peptide sequences and small synthetic and natural amphiphiles, in which weaker interactions such as hydrophobicity and chirality are likely to stabilize a larger number of metastable transient states, other polymorphic transitions have been reported.[24–30] Nonetheless, to the best of our knowledge, no reports exist on polypeptides or proteins, in which all the intermediate polymorphic steps have been described within the same single system from the early aggregation into isotropic-like micelles to the final mature fibrils. This would include the identification of distinct protofilaments, their aggregation into ribbonlike structures, the twisting of the ribbons, the coiling of the ribbon into helical topologies, and their final closure into nanotube-like structures. Here, we show that all these transient states can be resolved as a function of incubation time, provided that a sufficient time resolution and long (four weeks) incubation times are used. We use as a model system the end-capped heptapeptide CH_3CONH-βAβAKLVFF-$CONH_2$ (CapFF, Scheme 1), modified from the Aβ(16–20) fragment KLVFF.[31,32] Although we have already shown the morphological transition of CapFF from twisted ribbons—stabilized by the aromatic stacking interactions of phenylalanine residues—to nanotubes, the latter promoted by an increase of the ionic strength,[26] here we show a much richer polymorphic kinetic evolution involving at least six different structural intermediates.

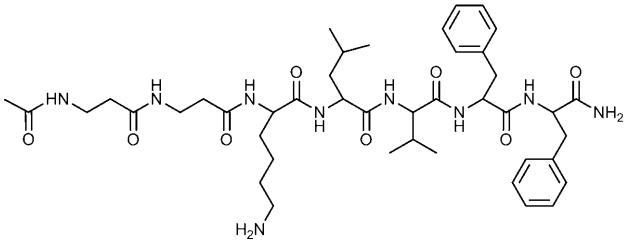

Scheme 1. Chemical structure of the CapFF heptapeptide.

The AFM images of 0.5 wt% CapFF in aqueous solution after 10 min and 5 h of incubation at room temperature and the corresponding height distributions are shown in Figure 1. At the very short incubation time of 10 min only very small spherical-like aggregates (Figure 1a) with a height of 1.5 nm (Figure 1b) were formed. These aggregates appear very

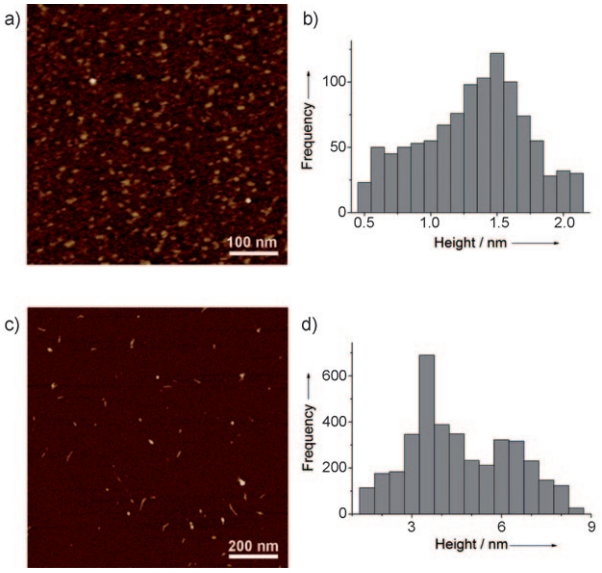

Figure 1. a) AFM image of CapFF aggregation after 10 min of incubation at 25 °C. b) Height distribution of the oligomers observed after 10 min at 25 °C. c) AFM image after 5 h of incubation of the CapFF at 25 °C. d) Height distribution of the short protofilaments observed after 5 h of incubation at 25 °C.

[*] Dr. J. Adamcik, Dr. S. Bolisetty, Prof. R. Mezzenga
Food & Soft Materials Science, Institute of Food Nutrition & Health, ETH Zürich, LFO23
Schmelzbergstrasse 9, 8092 Zürich (Switzerland)
E-mail: raffaele.mezzenga@agrl.ethz.ch
Dr. V. Castelletto, Prof. I. W. Hamley
Department of Chemistry, University of Reading
Reading RG6 6AD (U.K.)
E-mail: i.w.hamley@reading.ac.uk

Supporting information for this article is available on the WWW under http://dx.doi.org/10.1002/anie.201100807.

similar to the small oligomers recently predicted to be precursors of individual protofilaments.[33] With an increase of incubation time to 5 h the formation of short protofilaments could be observed (Figure 1c). The protofilaments appear to have a clear elongated shape and higher aspect ratio than the oligomers. The height was in the range from 1.5 to 8 nm with two peaks in the distribution, one dominant, centered at 3.5 nm, and another, half as intense, centered at 6–7 nm (Figure 1d).

The 1:2 ratio of the two height peaks (3.5 and 7 nm) and their respective intensities are both a clear indication that at this incubation time, protofilaments that have not yet developed to their final length start to touch and overlap because of hydrophobic interactions. Figure 2 contains AFM

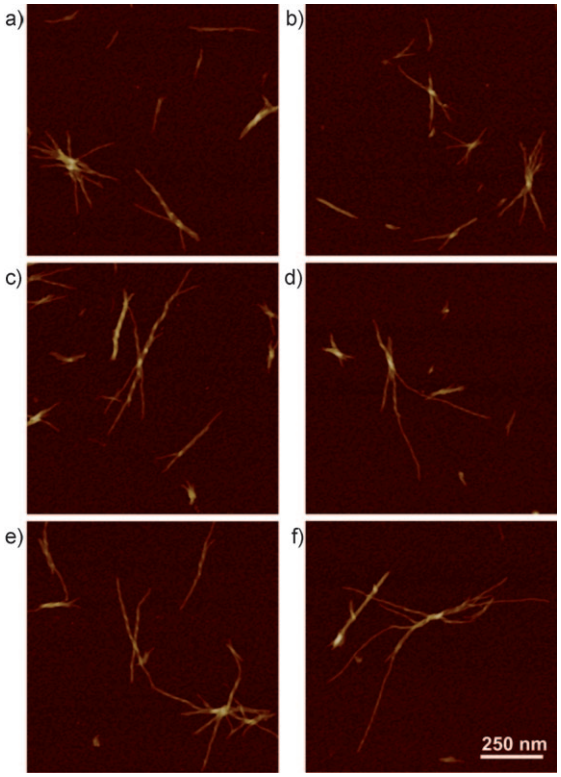

Figure 2. AFM images of CapFF aggregation after 10 h of incubation at 25 °C. The crossing of distinct filaments into multistranded fibrils and the twisting of the fibrils is clearly resolved in (a–f).

images of the intermediate states of fibril formation after 10 h of incubation. The attachment of longer single protofilaments to form a single multistranded early fibril and the initial stage of the twist can clearly be resolved. FTIR spectroscopy (Figure S1 in the Supporting Information) confirms the development during the same incubation time of a peak at 1625 cm^{-1} associated with β sheets. This mechanism of attachment and twisting is very similar to that observed in the formation of β-lactoglobulin multistranded amyloid fibrils.[23]

After 24 h of incubation the formation of twisted fibrils with regular periodicity was complete (Figure 3a–d). The cross-section indicates unambiguously that the fibrils form a twisted ribbon because of the zigzag height profile highlighted in Figure 3e. The contour length of the fibrils increases up to

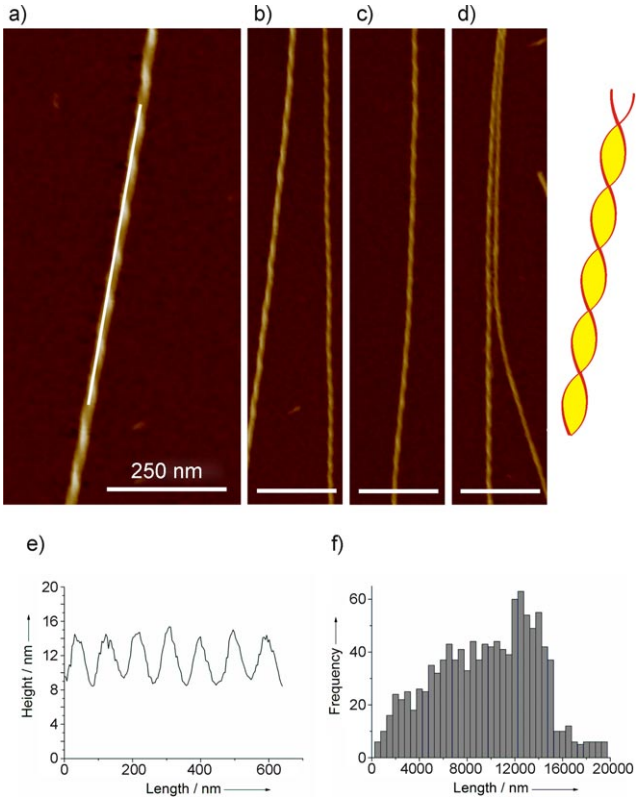

Figure 3. a–d) AFM images of twisted ribbons observed after 24 h of incubation at 25 °C; the scale bars are 250 nm. e) Height profile acquired along the portion of the contour length of the fibril shown in white in part (a). f) The contour length distribution of twisted ribbons observed after 24 h of incubation at 25 °C.

several micrometers (Figure 3f). Different heights for the fibrils can be resolved: for example, the fibrils shown in Figure 3 with maximum height of 7, 10, and 15 nm, have a periodicity of (33 ± 4), (54 ± 5), and (95 ± 10) nm, respectively. If we assume the hypothetical height h of individual protofilaments to be around 3.5 nm (Figure 1d), we can argue that the fibrils 7, 10, and 15 nm in height are made up of $n = 2$, $n = 3$, and $n = 4$ protofilaments, respectively. The pitch p, then obeys well the relationship $p \approx (n-1)d$, where d is the minimum observable pitch ($n = 2$) predicted for twisted ribbon amyloid fibrils.[8]

Helical ribbons were also observed to coexist with the twisted ribbons (Figure 4a–d). The cross-section of the helical ribbons is different from that of twisted ribbons, as revealed once again by the height profile (Figure 4e). Their contour length is similar to that of twisted ribbons (Figure 4f). Different heights of 7, 10, and 12 nm were observed. As can be seen, height maxima do not have a sharp profile, but rather a plateau of width s, where s is related to the real width of the ribbon w by $s = w/\sin(\gamma)$ and γ is the tilt angle of the helical ribbon edges with respect to the fibril axis. By measuring the average width $s = (90 \pm 10)$ nm for the ribbon in the half-height of the cross-section (Figure 4e) and measuring a tilt angle $\gamma = (30 \pm 5)°$, one easily finds a typical width of 45 nm for helical ribbons. Because this greatly exceeds the maximum height observed for twisted ribbons, these topological details

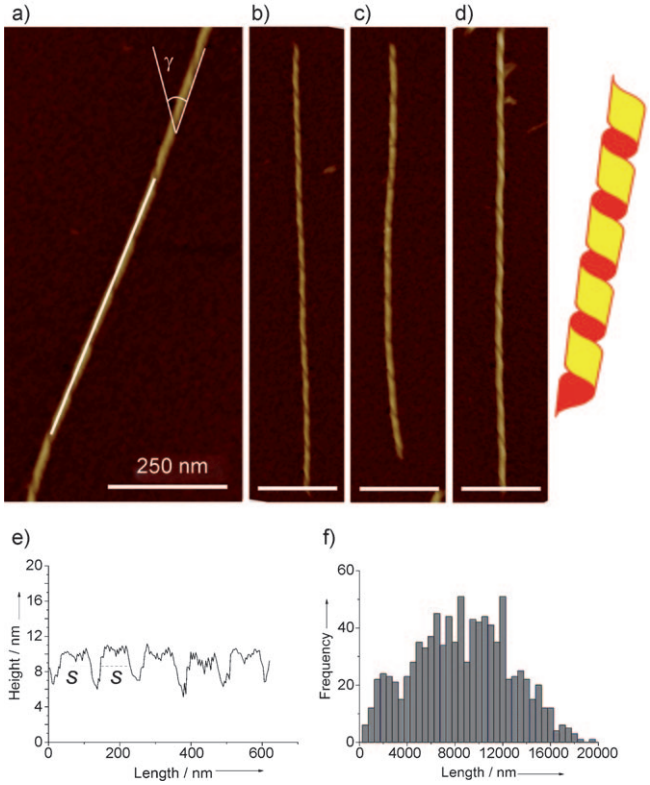

Figure 4. a–d) AFM images of helical ribbons which co-exist with twisted ribbons after 24 h of incubation at 25 °C; the scale bars are 250 nm. e) Height profile acquired along the portion of the contour length of the fibril shown in white in part (a). f) The contour length distribution of helical ribbons observed after 24 h of incubation at 25 °C.

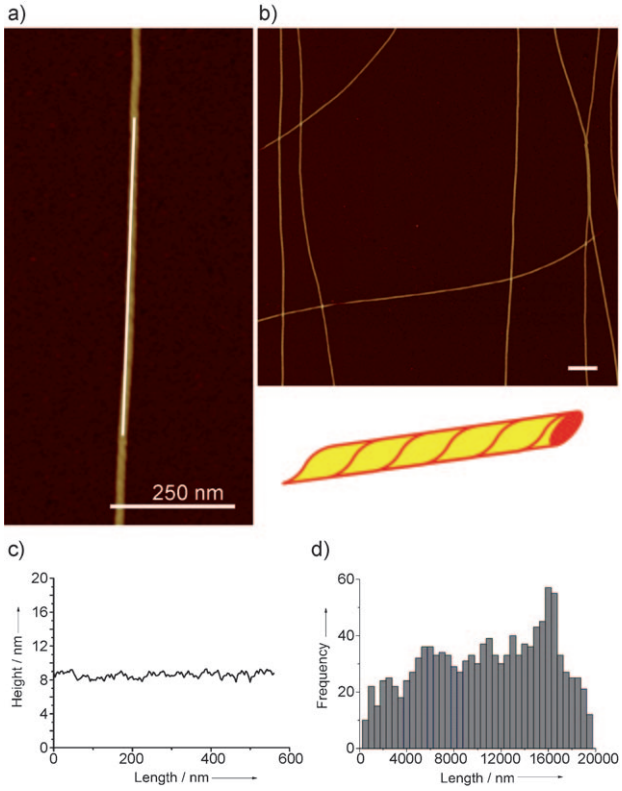

Figure 5. a,b) AFM images of nanotubes observed after 28 days of incubation at 4 °C; the scale bars are 250 nm. c) Height profile acquired along the portion of the contour length of the fibril shown in white in part (a). d) The contour length distribution of nanotubes observed after 28 days of incubation at 4 °C.

add further evidence that helical ribbons are a polymorphic state characteristic of fibrils that have achieved a greater lateral growth predominantly at later stages of fibrillation.

Following 24 h of incubation at room temperature, the heptapeptide solutions were then cooled to 4 °C and incubated at this temperature for 28 days. Figure 5 shows typical AFM images of samples incubated under these conditions. Periodic features cannot be resolved along the contour length of the fibrils, which appear to have reached a uniform cross-section, as also revealed by the constant height profile in Figure 5c.

Because the height is very close to that of the helical ribbons, it is straightforward to conclude that these objects are nanotube-like fibrils arising from the closure of the helical ribbons. Again, the contour length of the nanotubes is in the same range as for helical ribbons (Figure 5d).

Small-angle X-ray scattering (SAXS) confirmed that the cylinders are hollow (Figure 6). The scattering data acquired on 0.1 wt% dispersions of nanotubes after subtraction of water and capillary background, were fitted using the form of a hollow cylinder in the q range from 0.01 to 0.2 Å^{-1}. In the low q region the q^{-1} slope characteristic of rigid elongated objects can be recognized, whereas at higher values of q the intensity distribution corresponds to the cross-section of polydisperse hollow cylinders.

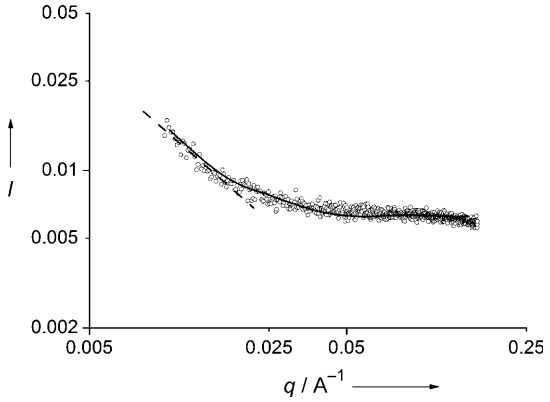

Figure 6. SAXS intensities I versus scattering vector q for the hollow nanotubes observed after 28 days of incubation. The circles are the measured scattering data and the solid line is the fit by a form factor of a polydisperse hollow cylinder. The dashed line is the asymptotic slope of −1 expected for rigid objects at low q.

The parameters used for the fitting yield 10 nm for the outer diameter of the cylinder, a shell thickness of 1.7 nm, and a polydispersity of 0.2. The matching of the external diameter fitting value and the height measured by AFM (Figure 5c) is remarkable. Further evidence for the hollow cylinders based on cryoTEM is given in the Supporting Information.

In our previous work,[26] we reported on the formation of CapFF nanotubes in the presence of NaCl, which allowed considerable screening of the electrostatic charges necessary to close the ribbon intermediates into nanotubes. CapFF has only one charge because of the presence of the lysine residue, the capped end groups are uncharged. Therefore, even at zero salt concentration, as in the present case, the nanotubes can still form, provided that sufficiently long time is allowed for this polymorphic change.

The relative populations of twisted ribbons, helical ribbons, and nanotubes at the different incubation times considered herein are summarized in Figure 7a. Figure 7b displays the time-dependent polymorphic changes resolved for CapFF.

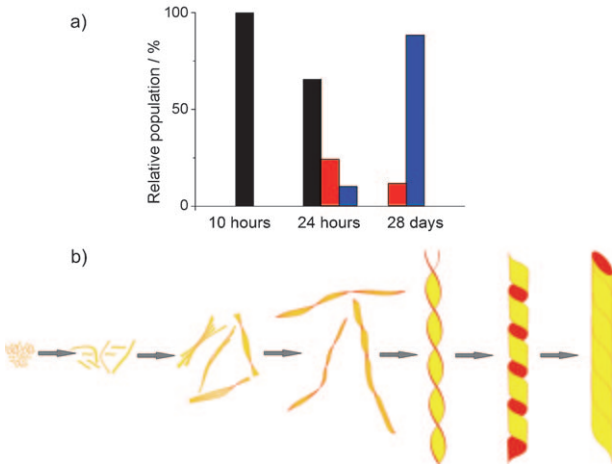

Figure 7. a) The relative populations of twisted ribbons (black), helical ribbons (red), and nanotubes (blue) at 10 h, 24 h, and 28 days of incubation. b) Time-dependent polymorphic changes in CapFF fibrillation.

It can be concluded that the fibrillation process proceeds through the states of twisted ribbons, helical ribbons, and nanotubes with increasing incubation time (Figure 7b). Although individual structural transitions among those identified here have been reported in separate studies on peptide and protein fibrillation, the entire kinetic evolution from the early states of oligomeric aggregation to the final nanotube morphologies is demonstrated here for the first time on a single peptide system, a heptapeptide derived from the Aβ(16–20) fragment. These results bring further structural insight into the fibrillation process of short polypeptides and is a meaningful model to interpret the more complex fibrillation processes in larger proteins and peptides typical of systemic amyloid diseases.

Received: January 31, 2011
Published online: April 29, 2011

Keywords: atomic force microscopy · helical structures · nanotubes · peptides · single-molecule studies

[1] F. Chiti, C. M. Dobson, *Annu. Rev. Biochem.* **2006**, *75*, 333–366.
[2] F. Chiti, C. M. Dobson, *Nat. Chem. Biol.* **2009**, *5*, 15–22.
[3] T. P. Knowles, A. W. Fitzpatrick, S. Meehan, H. R. Mott, M. Vendruscolo, C. M. Dobson, M. E. Welland, *Science* **2007**, *318*, 1900–1903.
[4] C. M. Dobson, *Nature* **2003**, *426*, 884–890.
[5] B. Caughey, P. T. Lansbury, *Annu. Rev. Neurosci.* **2003**, *26*, 267–298.
[6] R. Nelson, M. R. Sawaya, M. Balbirnie, A. Ø. Madsen, C. Riekel, R. Grothe, D. Eisenberg, *Nature* **2005**, *435*, 773–778.
[7] I. W. Hamley, *Angew. Chem.* **2007**, *119*, 8274–8295; *Angew. Chem. Int. Ed.* **2007**, *46*, 8128–8147.
[8] J. Adamcik, J. M. Jung, J. Flakowski, P. De Los Rios, G. Dietler, R. Mezzenga, *Nat. Nanotechnol.* **2010**, *5*, 423–428.
[9] A. Aggeli, M. Bell, N. Boden, L. Carrick, C. W. G. Fishwick, P. J. Mawer, S. E. Radford, A. E. Strong, *J. Am. Chem. Soc.* **2003**, *125*, 9619–9628.
[10] A. T. Petkova, Y. Ishii, J. J. Balbach, O. N. Antzutkin, R. D. Leapman, F. Delaglio, R. Tycko, *Proc. Natl. Acad. Sci. USA* **2002**, *99*, 16742–16747.
[11] A. T. Petkova, R. D. Leapman, Z. Guo, W. M. Yau, M. P. Mattson, R. Tycko, *Science* **2005**, *307*, 262–265.
[12] F. Chiti, P. Webster, N. Taddei, A. Clark, M. Stefani, G. Ramponi, C. M. Dobson, *Proc. Natl. Acad. Sci. USA* **1999**, *96*, 3590–3594.
[13] J. van Gestel, S. W. de Leeuw, *Biophys. J.* **2007**, *92*, 1157–1163.
[14] E. Gazit, *FEBS J.* **2005**, *272*, 5971–5978.
[15] R. Oda, I. Huc, M. Schmutz, S. J. Candau, F. C. MacKintosh, *Nature* **1999**, *399*, 566–569.
[16] A. Aggeli, I. A. Nyrkova, M. Bell, R. Harding, L. Carrick, T. C. McLeish, A. N. Semenov, N. Boden, *Proc. Natl. Acad. Sci. USA* **2001**, *98*, 11857–11862.
[17] R. Paparcone, M. J. Buehler, *Appl. Phys. Lett.* **2009**, *94*, 243904.
[18] T. P. Knowles, T. W. Oppenheim, A. K. Buell, D. Y. Chirgadze, M. E. Welland, *Nat. Nanotechnol.* **2010**, *5*, 204–207.
[19] M. Reches, E. Gazit, *Science* **2003**, *300*, 625–627.
[20] S. Scanlon, A. Aggeli, *Nano Today* **2008**, *3*, 22–30.
[21] R. V. Ulijn, A. M. Smith, *Chem. Soc. Rev.* **2008**, *37*, 664–675.
[22] R. de La Rica, H. Matsui, *Chem. Soc. Rev.* **2010**, *39*, 3499–3509.
[23] S. Bolisetty, J. Adamcik, R. Mezzenga, *Soft Matter* **2011**, *7*, 493–499.
[24] E. T. Pashuck, S. I. Stupp, *J. Am. Chem. Soc.* **2010**, *132*, 8819–8821.
[25] V. Castelletto, I. W. Hamley, C. Cenker, U. Olsson, *J. Phys. Chem. B* **2010**, *114*, 8002–8008.
[26] V. Castelletto, I. W. Hamley, Ç. Cenker, U. Olsson, J. Adamcik, R. Mezzenga, J. F. Miravet, B. Escuder, F. Rodríguez-Llansola, *J. Phys. Chem. B* **2011**, *115*, 2107–2116.
[27] K. Lu, J. Jacob, P. Thiyagarajan, V. P. Conticello, D. G. Lynn, *J. Am. Chem. Soc.* **2003**, *125*, 6391–6393.
[28] L. Ziserman, H. Z. Lee, S. R. Raghavan, A. Mor, D. Danino, *J. Am. Chem. Soc.* **2011**, *133*, 2511–2517.
[29] R. Oda, F. Artzner, M. Laguerre, I. Huc, *J. Am. Chem. Soc.* **2008**, *130*, 14705–14712.
[30] M. S. Spector, A. Singh, P. B. Messersmith, J. M. Schnur, *Nano Lett.* **2001**, *1*, 375–378.
[31] M. J. Krysmann, V. Castelletto, A. Kelarakis, I. W. Hamley, R. A. Hule, D. J Pochan, *Biochemistry* **2008**, *47*, 4597–4605.
[32] V. Castelletto, I. W. Hamley, R. A. Hule, D. J. Pochan, *Angew. Chem.* **2009**, *121*, 2353–2356; *Angew. Chem. Int. Ed.* **2009**, *48*, 2317–2320.
[33] J. D. Schmit, K. Ghosh, K. Dill, *Biophys. J.* **2011**, *100*, 450–458.